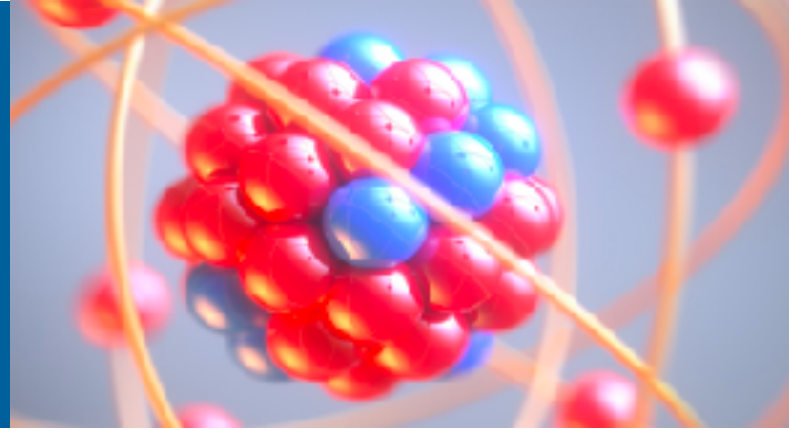


VARIATIONAL LEARNING QUANTUM WAVE FUNCTIONS



ALESSANDRO LOVATO



Trento Institute for
Fundamental Physics
and Applications



Mini-Workshop on Monte Carlo Methods
May 18, 2023

COLLABORATORS



C. Adams, **B. Fore**, **B. Hall**



G. Carleo, **G. Pescia**



J. Kim, M. Hjorth-Jensen



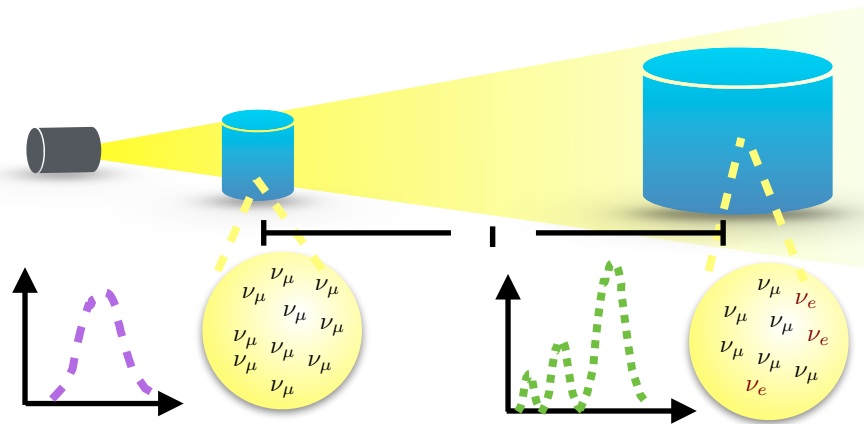
F. Pederiva, **M. Rigo**



N. Rocco

INTRODUCTION

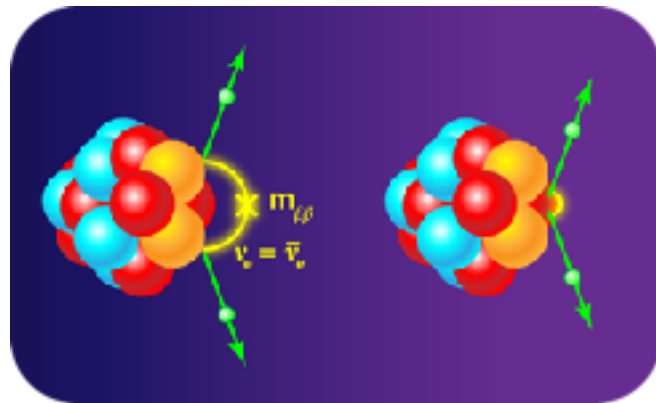
Oscillation parameters are measured by comparing the neutrino flux at near and far detectors



Accurate neutrino-nucleus scattering calculations are critical for the success of the experimental accelerator program

Credit: N. Rocco

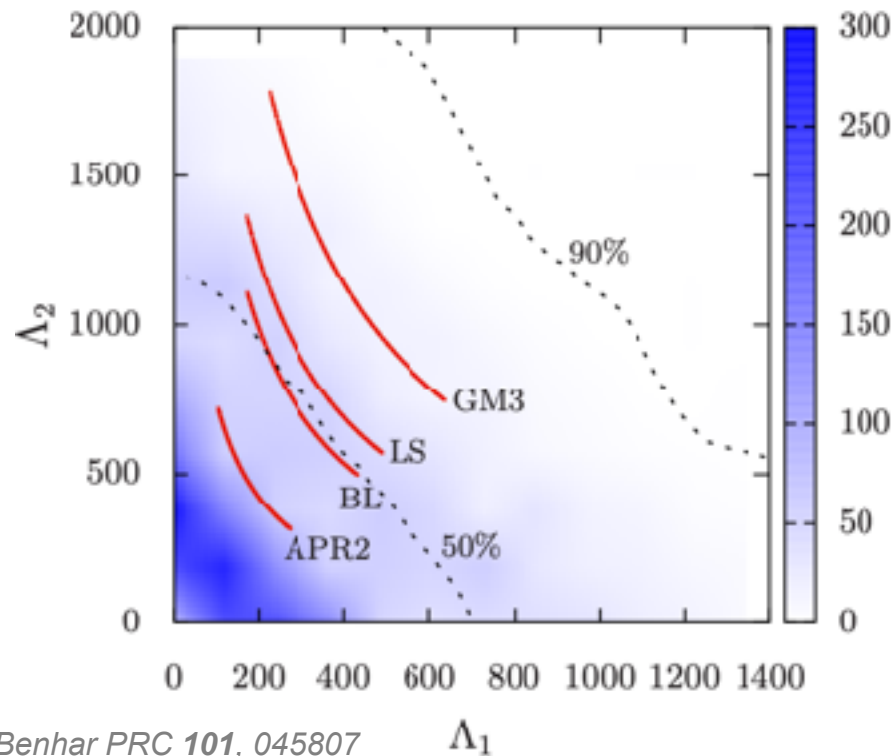
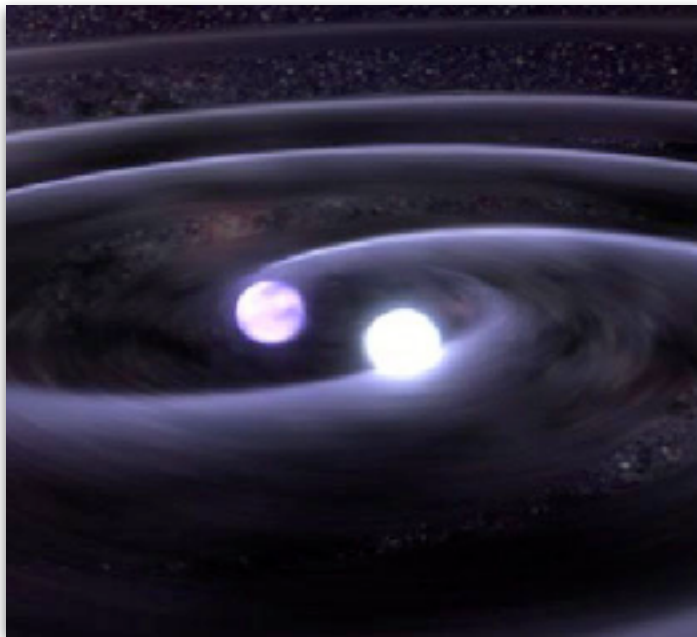
If observed, $0\nu\beta\beta$ would provide key insights into physics beyond the Standard Model



Relating experimental constraints on $0\nu\beta\beta$ decay rates to the neutrino masses requires quantitative estimates of nuclear matrix elements

INTRODUCTION

An accurate understanding of nuclear dynamics is critical for multi-messenger astronomy

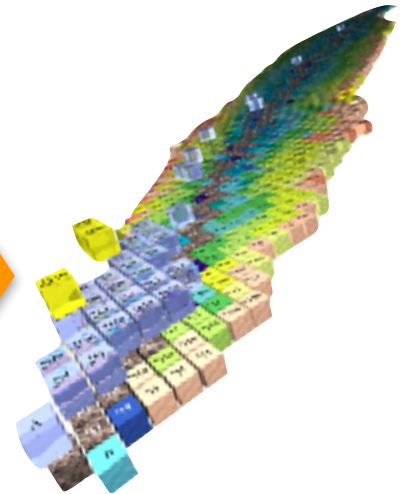
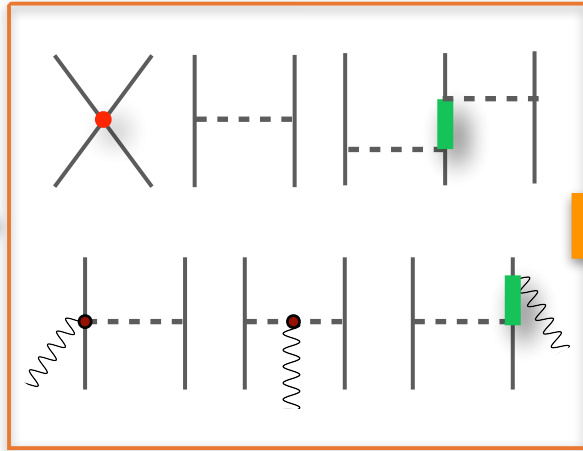
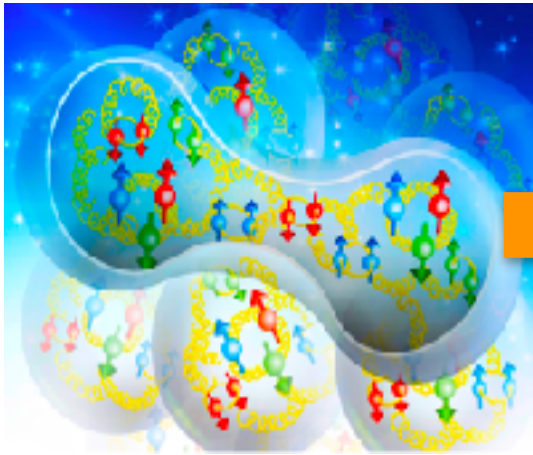


A. Sabatucci, O. Benhar PRC 101, 045807

THE NUCLEAR MANY-BODY PROBLEM

In the low-energy regime, quark and gluons are confined within hadrons and the relevant degrees of freedom are protons, neutrons, and pions

Effective field theories are the link between QCD and nuclear observables.



NUCLEAR MANY-BODY METHODS

Non relativistic many body theory aims at solving the many-body Schrödinger equation

$$H\Psi_0(x_1, \dots, x_A) = E_0\Psi_0(x_1, \dots, \dots, x_A) \quad \longleftrightarrow \quad x_i \equiv \{\mathbf{r}_i, s_i^z, t_i^z\}$$

- Nuclear potentials are non-perturbative and spin-isospin dependent

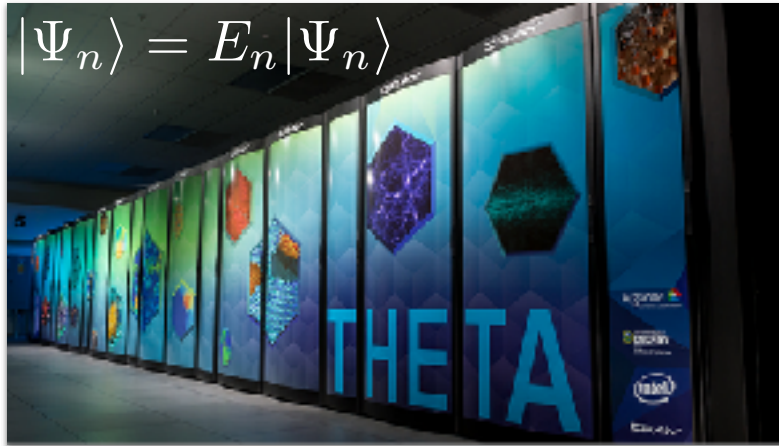
$$H = \sum_i \frac{\mathbf{p}_i^2}{2m} + \sum_{i<j} v_{ij} + \sum_{i<j<k} V_{ijk} \quad \left\{ \begin{array}{l} v_{ij} = \sum_{p=1}^{18} v^p(r_{ij}) O_{ij}^p \\ O_{ij}^{p=1,8} = (1, \sigma_{ij}, S_{ij}, \mathbf{L} \cdot \mathbf{S}) \times (1, \tau_{ij}) \end{array} \right.$$

- Nucleons are fermions, so the wave function must be anti-symmetric

$$\Psi_0(x_1, \dots, x_i, \dots, x_j, \dots, x_A) = -\Psi_0(x_1, \dots, x_j, \dots, x_i, \dots, x_A)$$

NUCLEAR MANY-BODY METHODS

- Hamiltonians and consistent currents are the main inputs to nuclear many-body methods
- These methods capitalize on high-performance computers to solve the Schrödinger equation with controlled approximation



- Nuclear many-body calculations are continually battling against the “curse of dimensionality,” the rapid growth with complexity of computational resources needed.

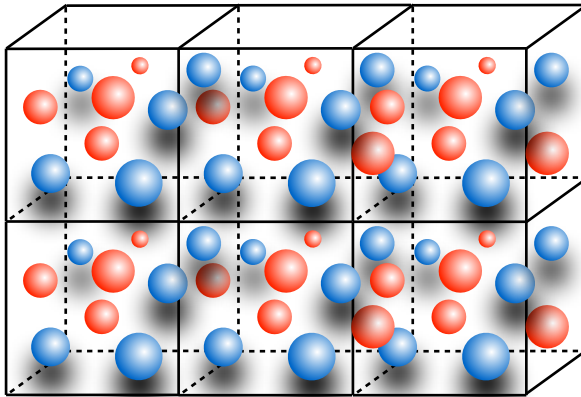
HARTREE-FOCK APPROXIMATION

Mean field approaches: the ground-state wave function is a single Slater determinant

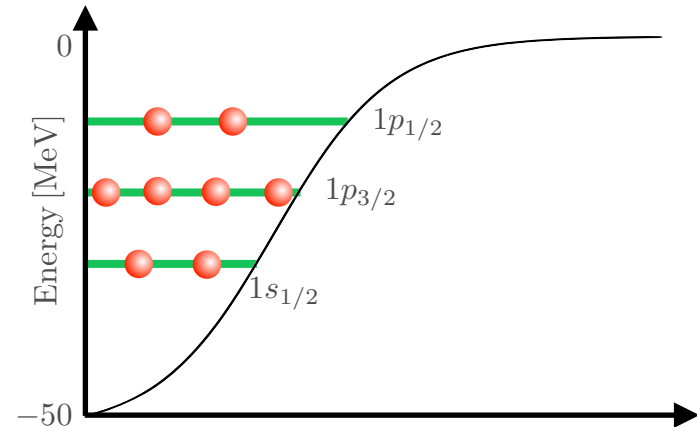
$$\Phi_0(\mathbf{r}_1, \mathbf{s}_1; \dots; \mathbf{r}_A, \mathbf{s}_A) = \mathcal{A}[\phi_{n_1}(\mathbf{r}_1, \mathbf{s}_1) \dots \phi_{n_A}(\mathbf{r}_A, \mathbf{s}_A)]$$

The single-particle states are consistent with the symmetry of the problem

Infinite nucleonic matter



Finite nuclei — ^{16}O



CONFIGURATION-INTERACTION

The exact ground-state wave function can be expressed as a sum of Slater determinants

$$\Psi_0(x_1, \dots, x_A) = \sum_n c_n \Phi_n(x_1, \dots, x_A)$$

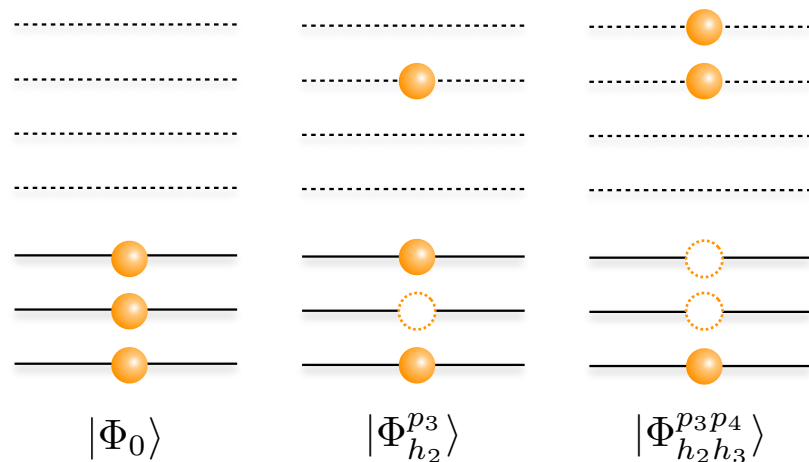
The occupation-number representation automatically encompasses the fermion antisymmetry

$$|\Psi_0\rangle = \sum_{h_1, \dots, p_1, \dots} c_{h_1, \dots, p_1, \dots}^{p_1, \dots} |\Phi_{h_1, \dots}^{p_1, \dots}\rangle$$

$$|\Phi_{h_1, \dots}^{p_1, \dots}\rangle = a_{p_1}^\dagger \dots a_{h_1} \dots |\Phi_0\rangle$$

The dimensionality explodes quickly

$$\binom{N}{A} = \frac{N!}{(N-A)!A!}$$



CONTINUUM QUANTUM MONTE CARLO

The trial wave function can be expanded in the set of the Hamiltonian eigenstates

$$|\Psi_T\rangle = \sum_n c_n |\Psi_n\rangle$$

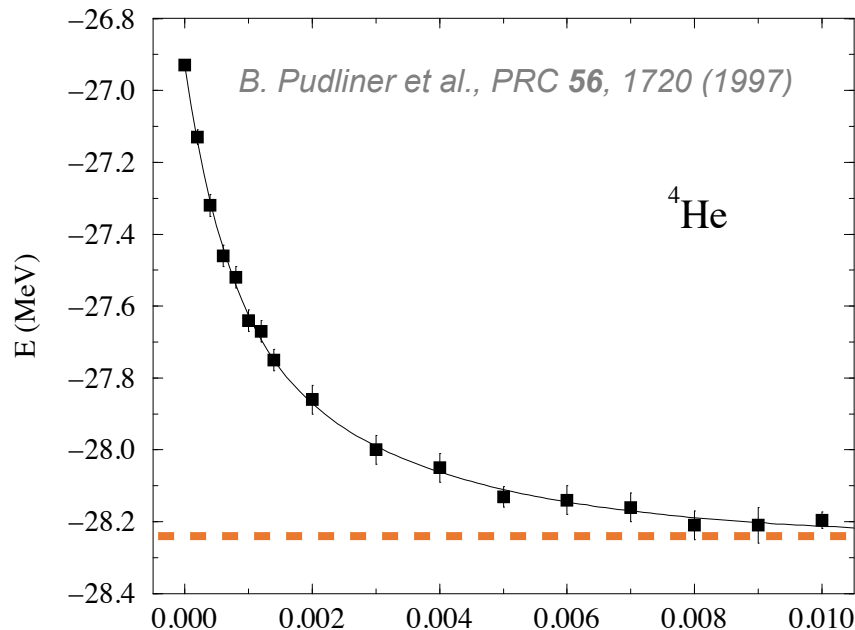
$$H|\Psi_n\rangle = E_n|\Psi_n\rangle$$

GFMC projects out the lowest-energy state using an imaginary-time propagation

$$\lim_{\tau \rightarrow \infty} e^{-(H-E_0)\tau} |\Psi_T\rangle = c_0 |\Psi_0\rangle$$

J. Carlson Phys. Rev. C 36, 2026 (1987)

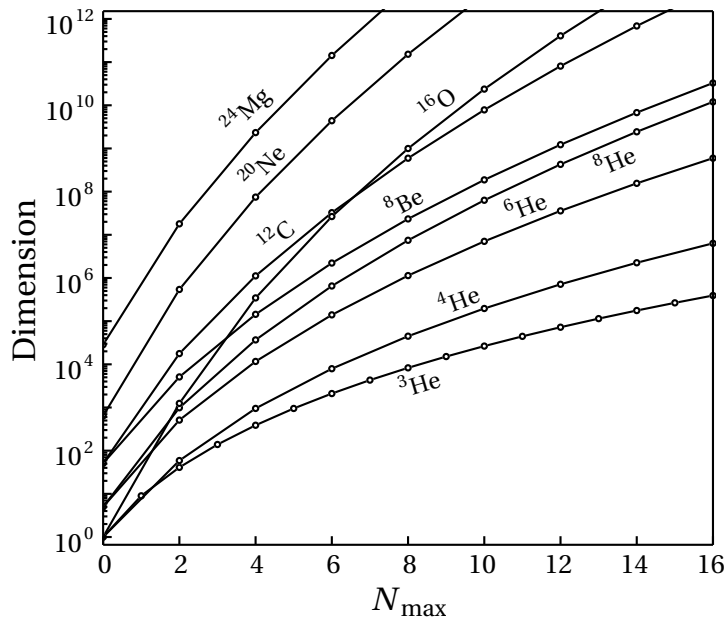
GFMC suffers from the fermion-sign problem, but it is “virtually exact” for light nuclear systems.



COURSE OF DIMENSIONALITY

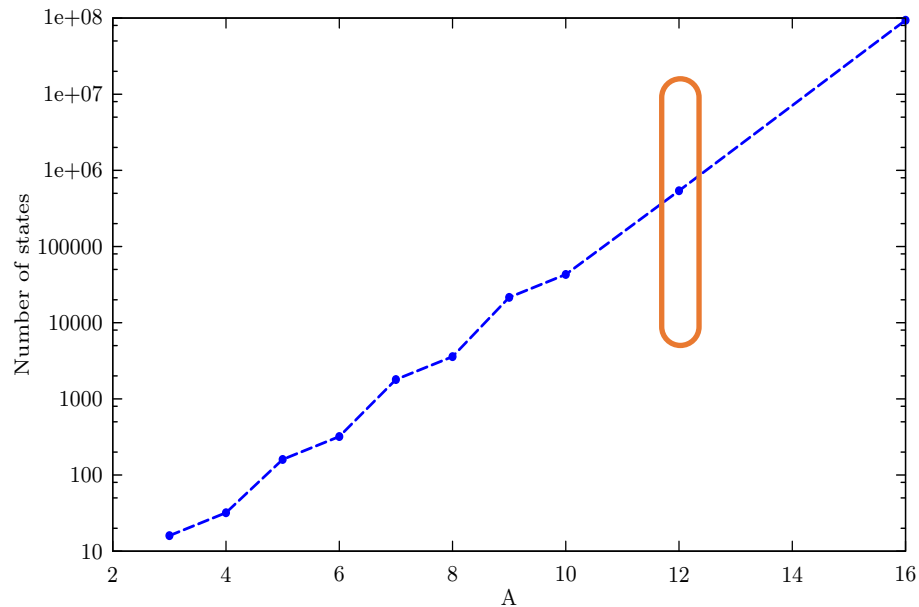
Configuration-Interaction

$$\Psi_0(x_1, \dots, x_A) = \sum_n c_n \Phi_n(x_1, \dots, x_A)$$

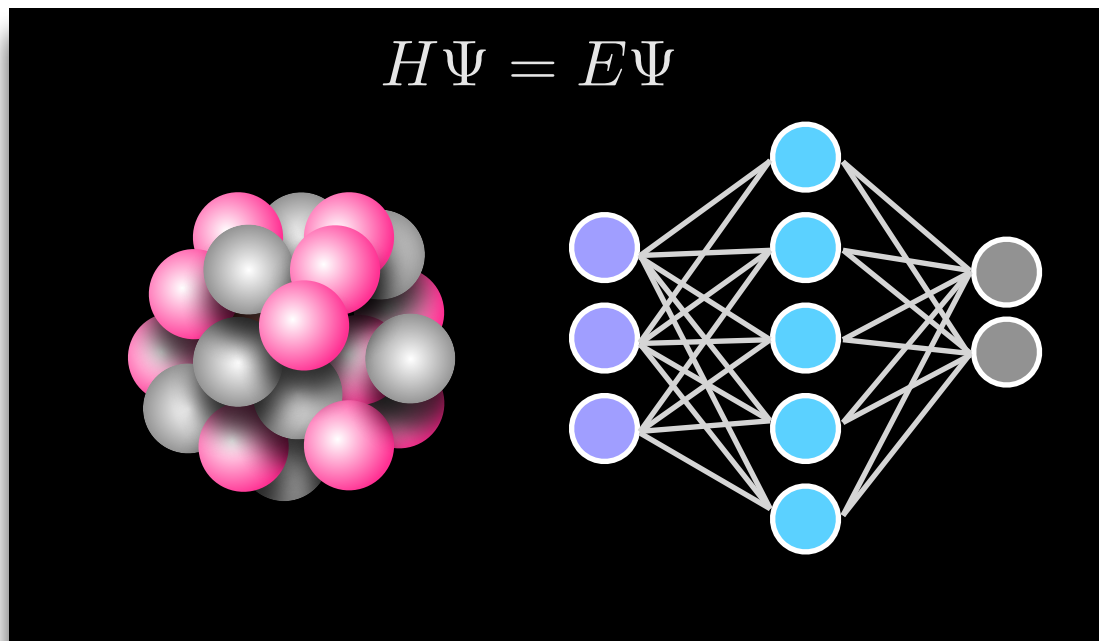


Green's function Monte Carlo

$$\lim_{\tau \rightarrow \infty} e^{-(H-E_0)\tau} |\Psi_T\rangle = c_0 |\Psi_0\rangle$$



NEURAL NETWORK QUANTUM STATES



NEURAL-NETWORK QUANTUM STATES

Let's take a step back: spin problem

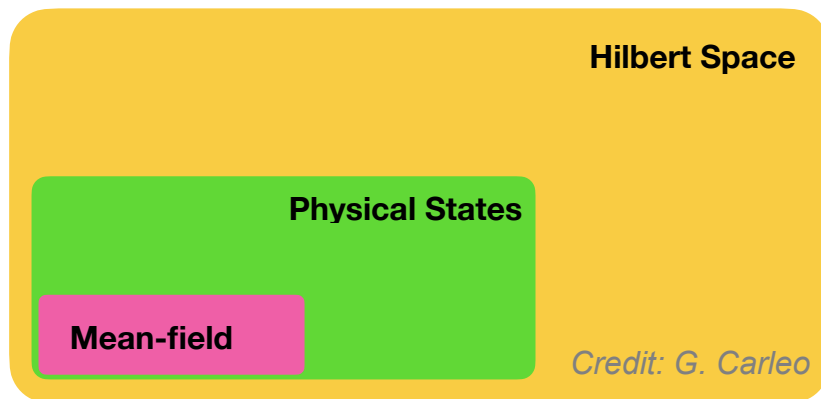


$$H_{TIF} = -h \sum_i \sigma_i^x - \sum_{\langle i,j \rangle} \sigma_i^z \sigma_j^z$$

Finding its exact solution of this equation is an **exponentially hard problem**

$$|\Psi\rangle = c_{\uparrow\uparrow\uparrow\dots} |\uparrow\uparrow\uparrow\dots\rangle + c_{\downarrow\uparrow\uparrow\dots} |\downarrow\uparrow\uparrow\dots\rangle + \dots + c_{\downarrow\downarrow\downarrow\dots} |\downarrow\downarrow\downarrow\dots\rangle$$

The majority of quantum states of physical interest have distinctive features and intrinsic structures



NEURAL-NETWORK QUANTUM STATES

$$\left\{ \begin{array}{l} c_{\uparrow\uparrow\uparrow\dots} \equiv \langle \uparrow\uparrow\uparrow \dots | \Psi \rangle \equiv \Psi(\uparrow\uparrow\uparrow \dots) \\ c_{\downarrow\uparrow\uparrow\dots} \equiv \langle \downarrow\uparrow\uparrow \dots | \Psi \rangle \equiv \Psi(\downarrow\uparrow\uparrow \dots) \\ c_{\downarrow\downarrow\downarrow\dots} \equiv \langle \downarrow\downarrow\downarrow \dots | \Psi \rangle \equiv \Psi(\downarrow\downarrow\downarrow \dots) \end{array} \right. \longleftrightarrow c_S \equiv \langle S | \Psi \rangle \equiv \Psi(S)$$

Artificial neural networks (ANNs) can compactly represent complex high-dimensional functions;

$$\Psi(S) \simeq \langle S | \hat{\Psi}(W) \rangle \equiv \hat{\Psi}(S; W)$$

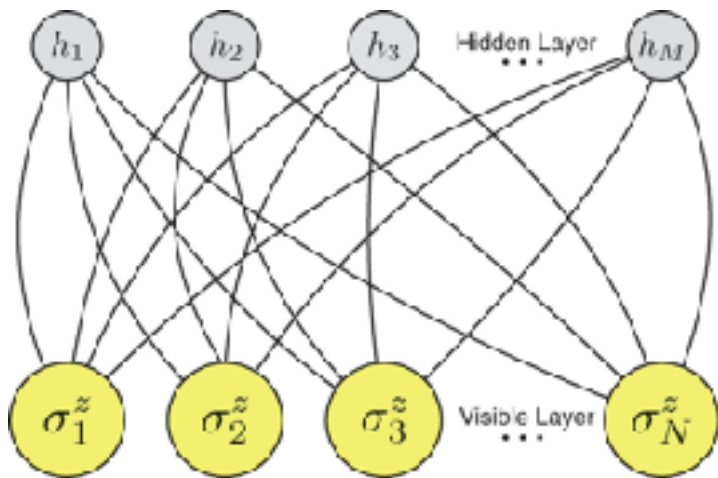
ANNs trained minimizing the energy, which is evaluated stochastically

$$E(W) = \frac{\langle \hat{\Psi}(W) | H | \hat{\Psi}(W) \rangle}{\langle \hat{\Psi}(W) | \hat{\Psi}(W) \rangle} \simeq \sum_{S_n} \frac{\langle S_n | H | \hat{\Psi}(W) \rangle}{\langle S_n | \hat{\Psi}(W) \rangle} \quad P(S_n) = |\langle S_n | \hat{\Psi}(W) \rangle|^2$$

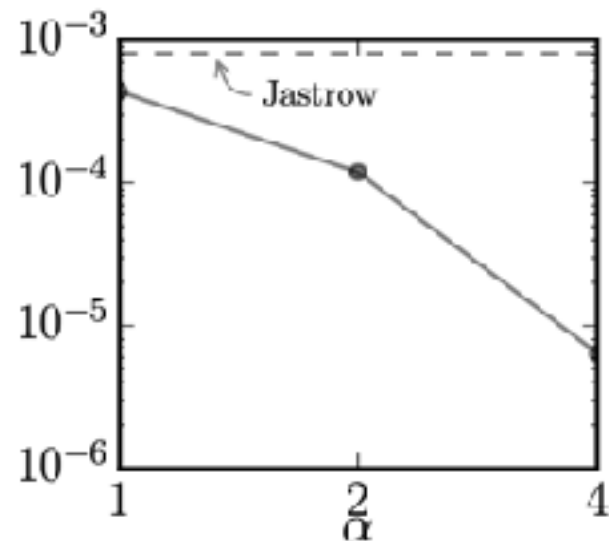
NEURAL-NETWORK QUANTUM STATES

Giuseppe Carleo and Mathias Troyer demonstrated that RBMs outperform traditional Jastrows

$$\hat{\Psi}(S; \mathcal{W}) = \sum_{\{h_i\}} e^{\sum_j a_j \sigma_j^z + \sum_i b_i h_i + \sum_{ij} W_{ij} h_i \sigma_j^z}$$



$$H_{TIF} = -h \sum_i \sigma_i^x - \sum_{\langle i,j \rangle} \sigma_i^z \sigma_j^z$$



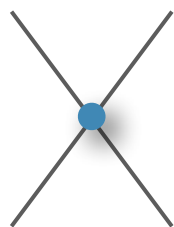
G. Carleo et al. *Science* **355**, 602 (2017)

PIONLESS EFT HAMILTONIAN

We take as input a LO pionless-EFT Hamiltonian that we contributed developing

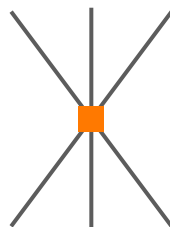
$$H_{LO} = - \sum_i \frac{\vec{\nabla}_i^2}{2m_N} + \sum_{i<j} v_{ij} + \sum_{i<j<k} V_{ijk}$$

- NN potential: fit to np scattering lengths and effective radii and the deuteron binding energy
- 3NF adjusted to reproduce the ^3H binding energy.



$$v_{ij}^{\text{CI}} = \sum_{p=1}^4 v^p(r_{ij}) O_{ij}^p,$$

$$O_{ij}^{p=1,4} = (1, \tau_{ij}, \sigma_{ij}, \sigma_{ij}\tau_{ij})$$



$$V_{ijk} = \tilde{c}_E \sum_{\text{cyc}} e^{-(r_{ij}^2 + r_{jk}^2)/R_3^2}$$

R. Schiavilla, AL, PRC 103, 054003(2021)

NEURAL SLATER-JASTROW ANSATZ

The ANN variational state is a product of mean-field state modulated by a flexible correlator factor

$$\Psi_{SJ}(X) = e^{J(X)} \Phi(X)$$

- The mean-field part is a Slater determinants of single-particle orbitals

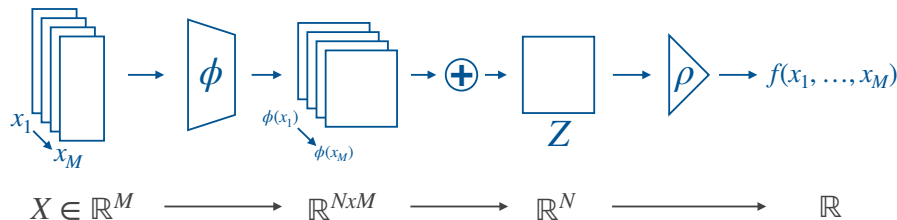
$$\det \begin{bmatrix} \phi_1(\mathbf{x}_1) & \phi_1(\mathbf{x}_2) & \cdots & \phi_1(\mathbf{x}_N) \\ \phi_2(\mathbf{x}_1) & \phi_2(\mathbf{x}_2) & \cdots & \phi_2(\mathbf{x}_N) \\ \vdots & \vdots & \ddots & \vdots \\ \phi_N(\mathbf{x}_1) & \phi_N(\mathbf{x}_2) & \cdots & \phi_N(\mathbf{x}_N) \end{bmatrix}$$

- Each orbital is a FFNN that takes as input

$$\bar{\mathbf{r}}_i = \mathbf{r}_i - \mathbf{R}_{CM}$$

- The Jastrow is a permutation-invariant function of the single-particle coordinates

$$J(X) = \rho_F \left[\sum_i \vec{\phi}_{\mathcal{F}}(\bar{\mathbf{r}}_i, \mathbf{s}_i) \right]$$



SAMPLING COORDINATES AND SPIN

The calculation of the observables involve integrating over 3A spatial and 2A spin-isospin variables

$$E_V = \frac{\langle \Psi_V | H | \Psi_V \rangle}{\langle \Psi_V | \Psi_V \rangle} = \frac{\sum_S \int dR |\Psi_V(R, S)|^2 \frac{\langle RS | H | \Psi_V \rangle}{\langle RS | \Psi_V \rangle}}{\sum_S \int dR |\Psi_V(R, S)|^2}.$$

We evaluate it stochastically using the Metropolis-Hastings Markov Chain Monte Carlo algorithm

$$\text{Spatial move} \longrightarrow P_R = \frac{|\Psi_V(R', S)|^2}{|\Psi_V(R, S)|^2} \quad \text{Spin-isospin move} \longrightarrow P_S = \frac{|\Psi_V(R, S')|^2}{|\Psi_V(R, S)|^2}$$

The observables are estimated by taking averages over the sampled configurations

$$\frac{\langle \Psi_V | O | \Psi_V \rangle}{\langle \Psi_V | \Psi_V \rangle} = \frac{1}{N_{\text{conf}}} \sum_{\{R, S\}} O_L(R, S) \longleftrightarrow P_V(R, S) = \frac{|\Psi_V(R, S)|^2}{\sum_S \int dR |\Psi_V(R, S)|^2}.$$

STOCHASTIC RECONFIGURATION

The ANN is trained by performing an imaginary-time evolution in the variational manifold

$$(1 - H\delta\tau)|\Psi_V(\mathbf{p}_\tau)\rangle \simeq \Delta p^0|\Psi_V(\mathbf{p}_\tau)\rangle + \sum_i \Delta p^i O^i |\Psi_V(\mathbf{p}_\tau)\rangle$$

During the optimization, then parameter are updated as

$$\mathbf{p}_{\tau+\delta\tau} = \mathbf{p}_\tau - \eta(S_\tau + \epsilon I)^{-1} \mathbf{g}_\tau$$

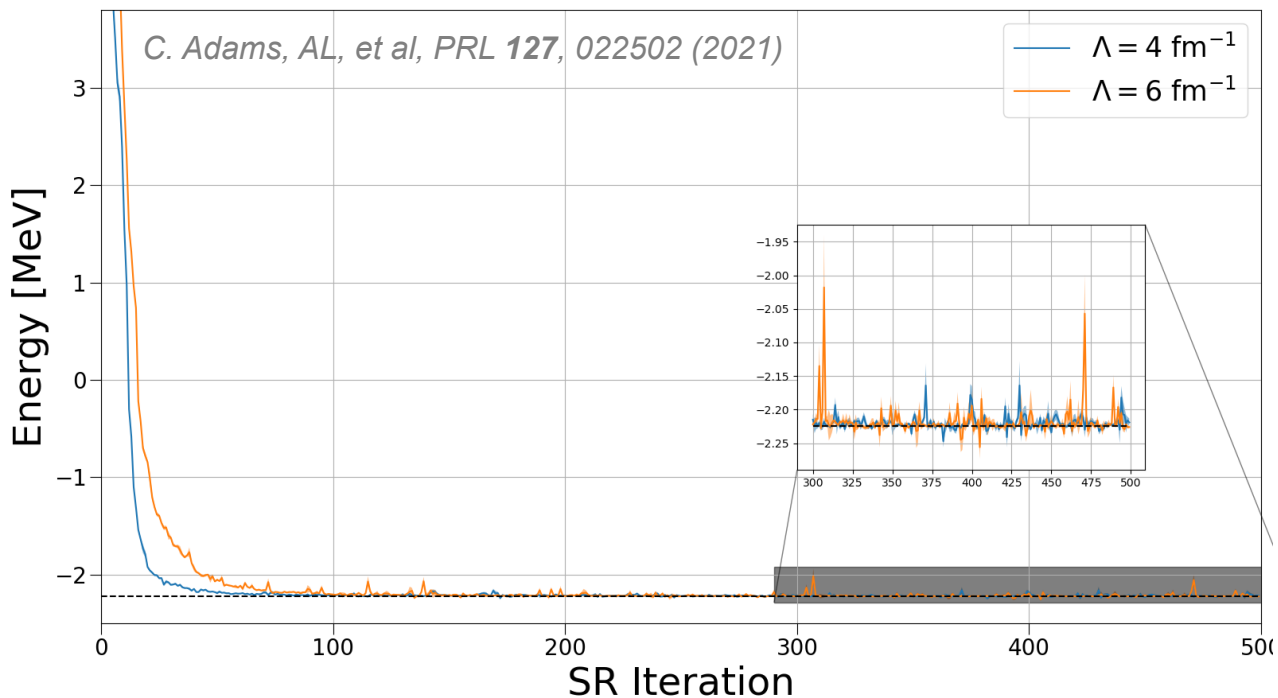
The gradient of the energy is supplemented by a quantum Fisher information pre-conditioner

$$\left\{ \begin{aligned} g_\tau^i &= 2\langle \Psi_V(\mathbf{p}_\tau) | O^i H | \Psi_V(\mathbf{p}_\tau) \rangle - 2\langle \Psi_V(\mathbf{p}_\tau) | H | \Psi_V(\mathbf{p}_\tau) \rangle \langle \Psi_V(\mathbf{p}_\tau) | O^i | \Psi_V(\mathbf{p}_\tau) \rangle \\ S_\tau^{ij} &= \langle \Psi_V(\mathbf{p}_\tau) | O^i O^j | \Psi_V(\mathbf{p}_\tau) \rangle - \langle \Psi_V(\mathbf{p}_\tau) | O^i | \Psi_V(\mathbf{p}_\tau) \rangle \langle \Psi_V(\mathbf{p}_\tau) | O^j | \Psi_V(\mathbf{p}_\tau) \rangle \end{aligned} \right.$$

S. Sorella, Phys. Rev. B **64**, 024512 (2001)

ADAPTIVE STOCHASTIC RECONFIGURATION

We use an adaptive learning rate with $10^{-7} < \eta < 10^{-2}$. It yields robust convergence patterns for all the nuclei and regulator choices that we have analyzed

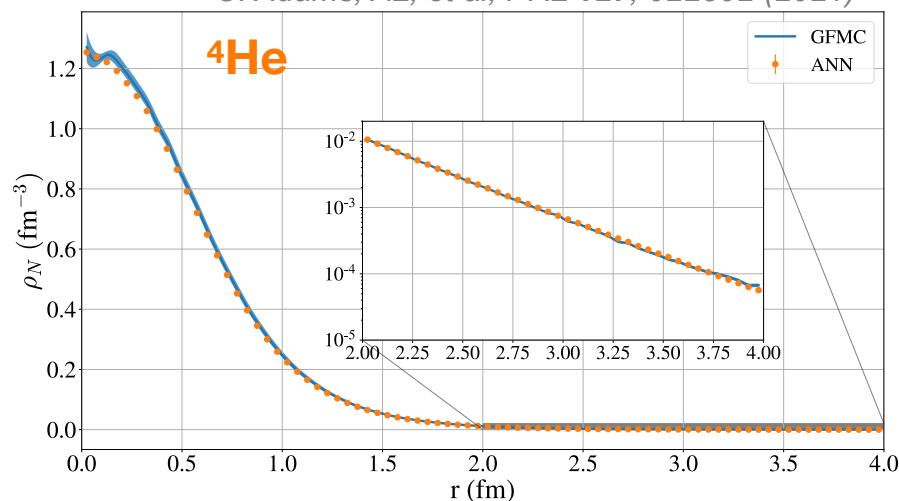
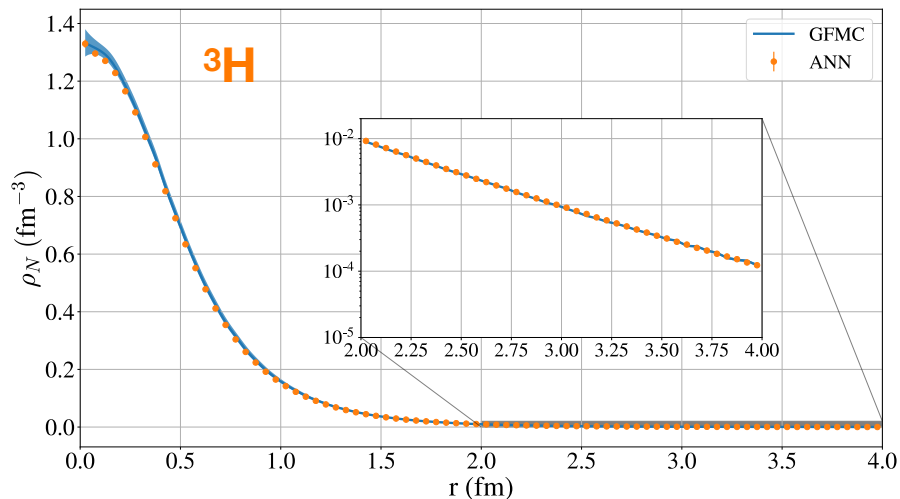


COMPARISON WITH QUANTUM MONTE CARLO

To further elucidate the quality of the ANN wave function we consider the point-nucleon density

$$\rho_N(r) = \frac{1}{4\pi r^2} \langle \Psi_V | \sum_i \delta(r - |\mathbf{r}_i^{\text{int}}|) | \Psi_V \rangle,$$

C. Adams, AL, et al, PRL 127, 022502 (2021)



Excellent agreement between the ANN and GFMC methods, which further corroborates the representative power of the ANN ansatz.

COMPARISON WITH QUANTUM MONTE CARLO

C. Adams, AL, et al, PRL 127, 022502 (2021)

- The ANN ansatz outperforms standard Jastrow correlations and encompasses the vast majority of spin-isospin correlations
- Remaining differences with the exact GFMC result are due to missing spin-isospin correlations

	Λ	VMC-ANN	VMC-JS	GFMC	GFMC _e
${}^2\text{H}$	4 fm ⁻¹	-2.224(1)	-2.223(1)	-2.224(1)	-
	6 fm ⁻¹	-2.224(4)	-2.220(1)	-2.225(1)	-
${}^3\text{H}$	4 fm ⁻¹	-8.26(1)	-7.80(1)	-8.38(2)	-7.82(1)
	6 fm ⁻¹	-8.27(1)	-7.74(1)	-8.38(2)	-7.81(1)
${}^4\text{He}$	4 fm ⁻¹	-23.30(2)	-22.54(1)	-23.62(3)	-22.77(2)
	6 fm ⁻¹	-24.47(3)	-23.44(2)	-25.06(3)	-24.10(2)

- The Jastrow ansatz cannot compensate the wrong nodes in the mean-field part of the wave function

$$\left\{ \begin{array}{l} \langle RS | \Psi_V^{\text{ANN}} \rangle = e^{\mathcal{U}(R,S)} \tanh[\mathcal{V}(R,S)] \langle RS | \Phi \rangle \\ \langle RS | \Phi \rangle = \begin{pmatrix} \langle s_1^z t_1^z | p \uparrow \rangle & \langle s_2^z t_2^z | p \uparrow \rangle & \langle s_3^z t_3^z | p \uparrow \rangle & \langle s_4^z t_4^z | p \uparrow \rangle \\ \langle s_1^z t_1^z | p \downarrow \rangle & \langle s_2^z t_2^z | p \downarrow \rangle & \langle s_3^z t_3^z | p \downarrow \rangle & \langle s_4^z t_4^z | p \downarrow \rangle \\ \langle s_1^z t_1^z | n \uparrow \rangle & \langle s_2^z t_2^z | n \uparrow \rangle & \langle s_3^z t_3^z | n \uparrow \rangle & \langle s_4^z t_4^z | n \uparrow \rangle \\ \langle s_1^z t_1^z | n \downarrow \rangle & \langle s_2^z t_2^z | n \downarrow \rangle & \langle s_3^z t_3^z | n \downarrow \rangle & \langle s_4^z t_4^z | n \downarrow \rangle \end{pmatrix} \end{array} \right.$$

HIDDEN NUCLEONS

The “hidden fermion” approach was recently introduced to model fermionic wave functions

$$\langle RS | \Psi_{HF} \rangle = \left(\begin{array}{cccc|cccc} \phi_1(x_1) & \phi_1(x_2) & \phi_1(x_3) & \phi_1(x_4) & \phi_1(y_1) & \phi_1(y_2) & \phi_1(y_3) & \phi_1(y_4) \\ \phi_2(x_1) & \phi_2(x_2) & \phi_2(x_3) & \phi_2(x_4) & \phi_2(y_1) & \phi_2(y_2) & \phi_2(y_3) & \phi_2(y_4) \\ \phi_3(x_1) & \phi_3(x_2) & \phi_3(x_3) & \phi_3(x_4) & \phi_3(y_1) & \phi_3(y_2) & \phi_3(y_3) & \phi_3(y_4) \\ \phi_4(x_1) & \phi_4(x_2) & \phi_4(x_3) & \phi_4(x_4) & \phi_4(y_1) & \phi_4(y_2) & \phi_4(y_3) & \phi_4(y_4) \\ \chi_1(x_1) & \chi_1(x_2) & \chi_1(x_3) & \chi_1(x_4) & \chi_1(y_1) & \chi_1(y_2) & \chi_1(y_3) & \chi_1(y_4) \\ \chi_2(x_1) & \chi_2(x_2) & \chi_2(x_3) & \chi_2(x_4) & \chi_2(y_1) & \chi_2(y_2) & \chi_2(y_3) & \chi_2(y_4) \\ \chi_3(x_1) & \chi_3(x_2) & \chi_3(x_3) & \chi_3(x_4) & \chi_3(y_1) & \chi_3(y_2) & \chi_3(y_3) & \chi_3(y_4) \\ \chi_4(x_1) & \chi_4(x_2) & \chi_4(x_3) & \chi_4(x_4) & \chi_4(y_1) & \chi_4(y_2) & \chi_4(y_3) & \chi_4(y_4) \end{array} \right)$$

Visible orbitals on visible coordinates

Visible orbitals on hidden coordinates

Hidden orbitals on visible coordinates

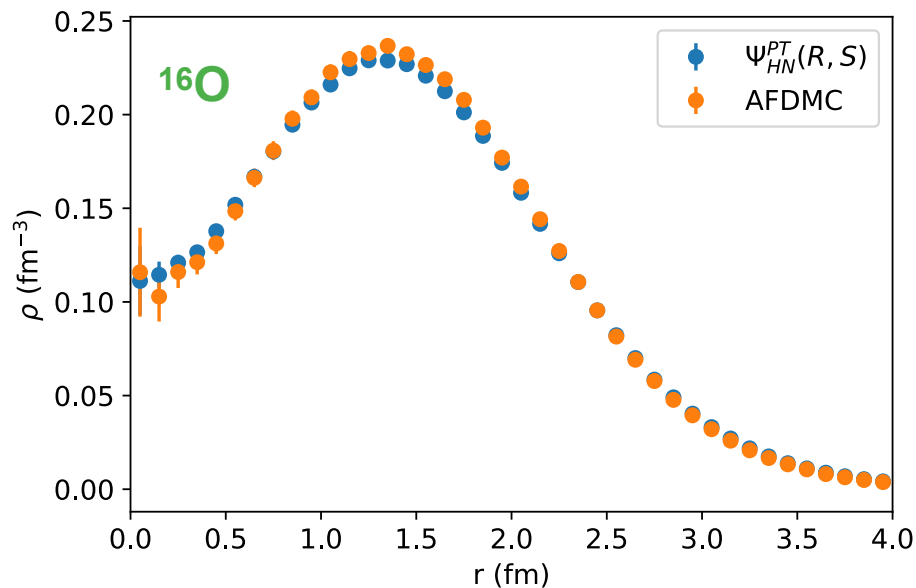
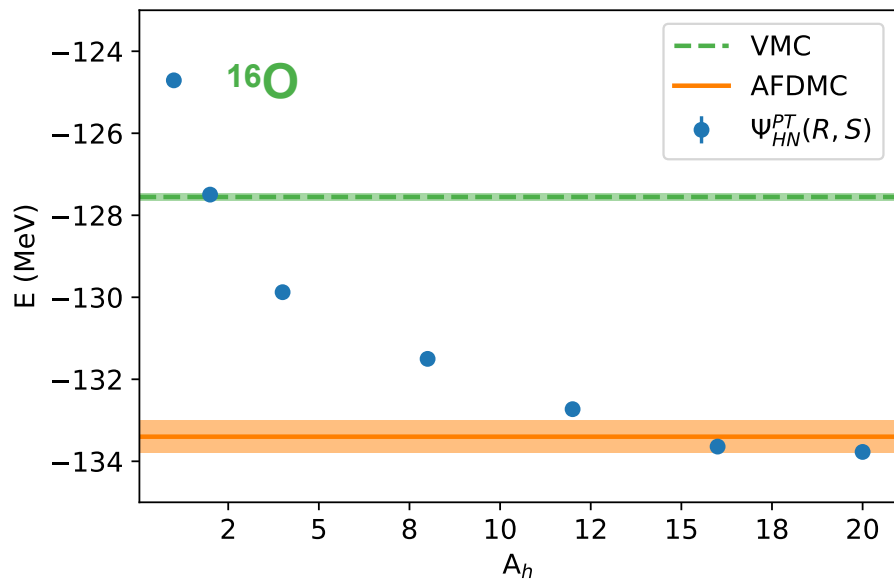
Hidden orbitals on hidden coordinates

J. R. Moreno, et al., PNAS 119 (32) e2122059119

NUCLEAR PHYSICS APPLICATIONS

We extend the reach of neural quantum states by computing the ground-state of ^{16}O

In addition to its ground-state energy, we evaluate the point-nucleon density of ^{16}O with $A_h=16$



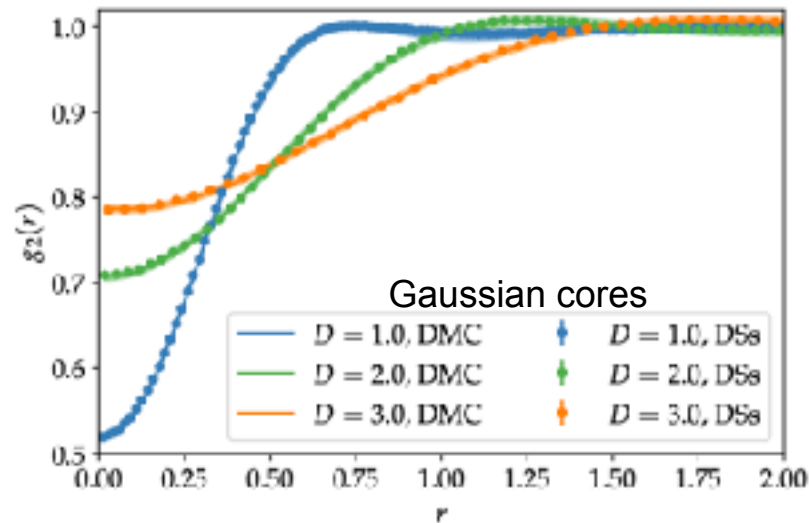
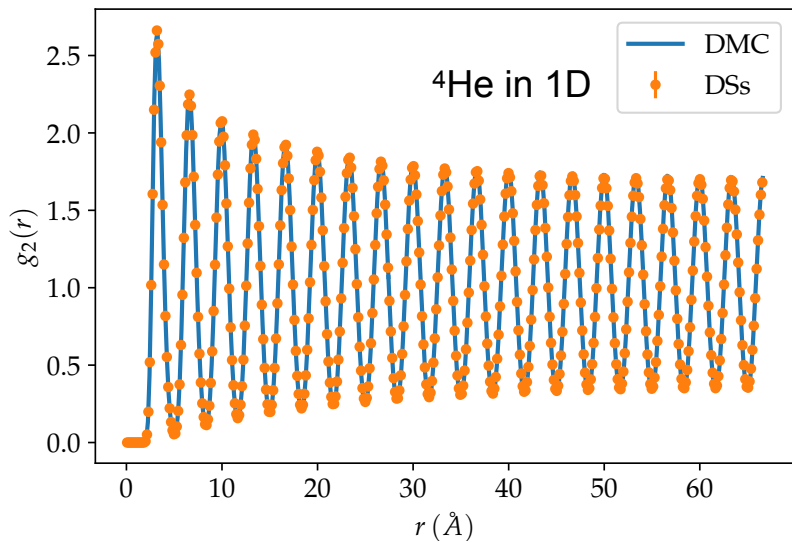
AL, et al., Phys.Rev.Res. 4 (2022) 4, 043178

INFINITE PERIODIC SYSTEMS

- We extended our approach to periodic systems, such as liquid ^4He and soft (gaussian) spheres

→ Periodic ANN by construction: $\mathbf{r}_i \longrightarrow \tilde{\mathbf{r}}_i = \left\{ \sin\left(\frac{2\pi}{L}\mathbf{r}_i\right), \cos\left(\frac{2\pi}{L}\mathbf{r}_i\right) \right\}$

→ Permutation invariant Deep-Sets ANN for computing bosons: $\Psi_V(R) = e^{\mathcal{U}(R)}$



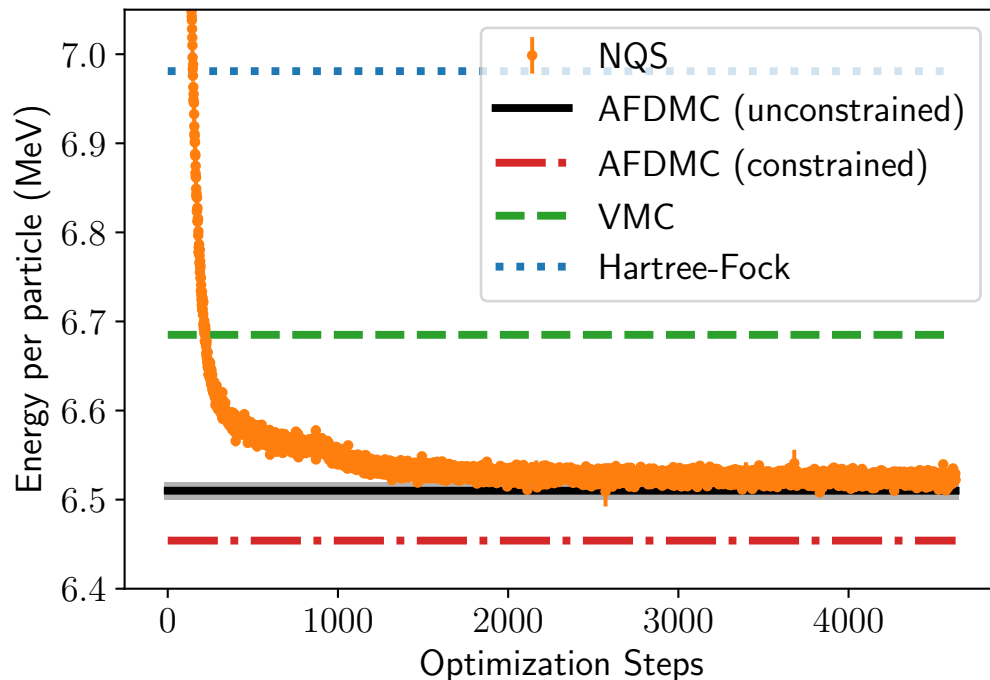
DILUTE NEUTRON MATTER

We have introduced a periodic hidden-nucleons ansatz to model low-density neutron matter

The NQS ansatz converges to the unconstrained AFDMC energy, using a fraction of the computing time

- NQS: 100 hours on NVIDIA-A100
- AFDMC: 1.2 million hours on Intel-KNL

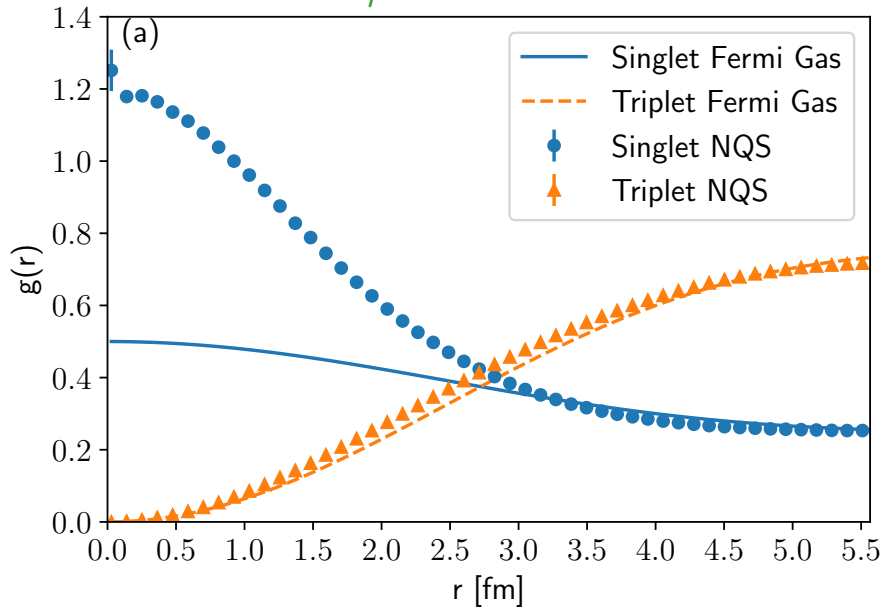
The hidden-nucleon ansatz captures the overwhelming majority of the correlation energy



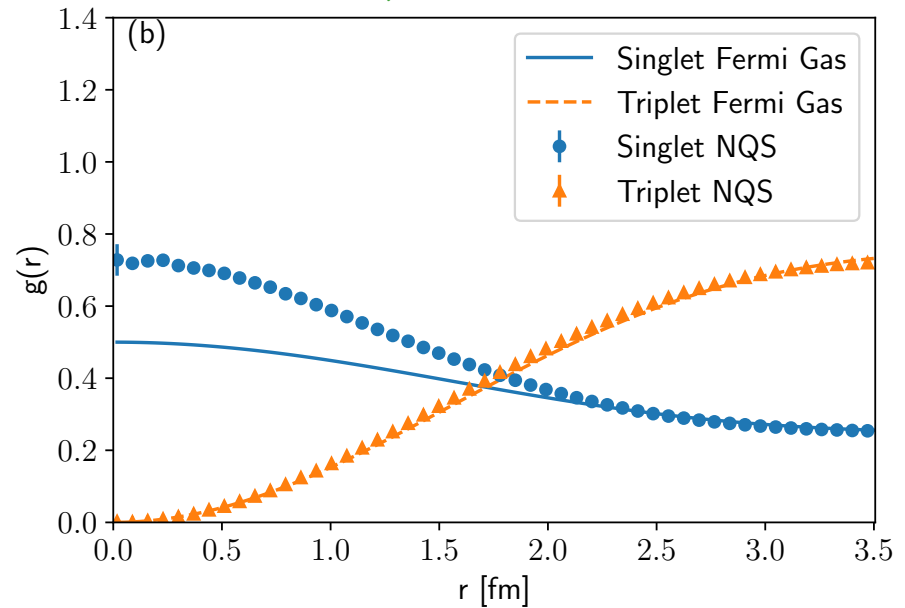
DILUTE NEUTRON MATTER

Low-density neutron matter is characterized by fascinating emergent quantum phenomena, such as the formation of Cooper pairs and the onset of superfluidity.

$$\rho = 0.01 \text{ fm}^{-3}$$



$$\rho = 0.04 \text{ fm}^{-3}$$



COLD FERMION GASES

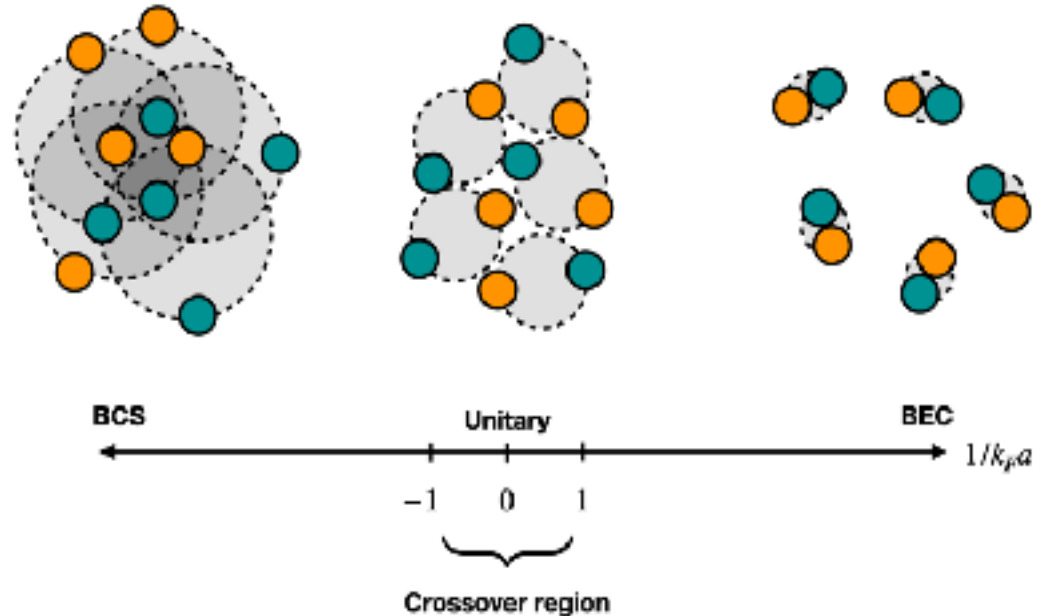
We have started using periodic-NQS to investigate properties of the two-components Fermi gas at unitarity and in the BCS- BEC crossover

- We model the 3D unpolarized gas of fermions with the Hamiltonian

$$H = -\frac{\hbar^2}{2m} \sum_i \nabla_i^2 + \sum_{ij} v_{ij}$$

- As with the two-body force, we take the Pöschl-Teller potential

$$v_{ij} = (s_i \cdot s_j - 1) V_0 \frac{\hbar^2}{2m} \frac{\mu^2}{\cosh^2(\mu r_{ij})}$$



COLD FERMION GASES

We consider periodic and NSQ ansätze of the general form

$$\Psi(X) = e^{J(X)} \Phi(X),$$

The antisymmetric part of the Slater-Jastrow (SJ) family of states can be written as

$$\Phi_{SJ}(X) = \det \begin{bmatrix} \phi_1(\mathbf{x}_1) & \phi_1(\mathbf{x}_2) & \cdots & \phi_1(\mathbf{x}_N) \\ \phi_2(\mathbf{x}_1) & \phi_2(\mathbf{x}_2) & \cdots & \phi_2(\mathbf{x}_N) \\ \vdots & \vdots & \ddots & \vdots \\ \phi_N(\mathbf{x}_1) & \phi_N(\mathbf{x}_2) & \cdots & \phi_N(\mathbf{x}_N) \end{bmatrix} ; \quad \phi_i^{PW}(\mathbf{x}_j) = e^{i\mathbf{k}_i \cdot \mathbf{r}_j} \langle \sigma_i | s_j \rangle ,$$

The nodal structure can be improved by means of general neural back-flow transformations

$$\mathbf{x}_i \longrightarrow \phi(\mathbf{x}_i; \mathbf{x}_{j \neq i})$$

COLD FERMION GASES

Inspired by quantum Monte Carlo studies of dilute neutron matter, we introduce a neural Pfaffian-Jastrow ansatz

$$\Phi_{PJ}(X) = \text{pf} \begin{bmatrix} 0 & \phi(\mathbf{x}_1, \mathbf{x}_2) & \cdots & \phi(\mathbf{x}_1, \mathbf{x}_N) \\ \phi(\mathbf{x}_2, \mathbf{x}_1) & 0 & \cdots & \phi(\mathbf{x}_2, \mathbf{x}_N) \\ \vdots & \vdots & \ddots & \vdots \\ \phi(\mathbf{x}_N, \mathbf{x}_1) & \phi(\mathbf{x}_N, \mathbf{x}_2) & \cdots & 0 \end{bmatrix}$$

In order for the above matrix to be skew-symmetric, the neural pairing orbitals are taken to be

$$\phi(\mathbf{x}_i, \mathbf{x}_j) = \eta(\mathbf{x}_i, \mathbf{x}_j) - \eta(\mathbf{x}_j, \mathbf{x}_i),$$

Example:

$$\text{pf} \begin{bmatrix} 0 & \phi_{12} & \phi_{13} & \phi_{14} \\ -\phi_{12} & 0 & \phi_{23} & \phi_{24} \\ -\phi_{13} & -\phi_{23} & 0 & \phi_{34} \\ -\phi_{14} & -\phi_{24} & -\phi_{34} & 0 \end{bmatrix} = \phi_{12}\phi_{34} - \phi_{13}\phi_{24} + \phi_{14}\phi_{23}$$

COLD FERMI GASES

We employ a permutation-invariant message-passing neural network to iteratively build correlations into new one-body and two-body features from the original “visible” features.

- Visible features

$$\mathbf{v}_i = (s_i),$$

$$\mathbf{v}_{ij} = (\mathbf{r}_{ij}, \|\mathbf{r}_{ij}\|, s_i s_j),$$

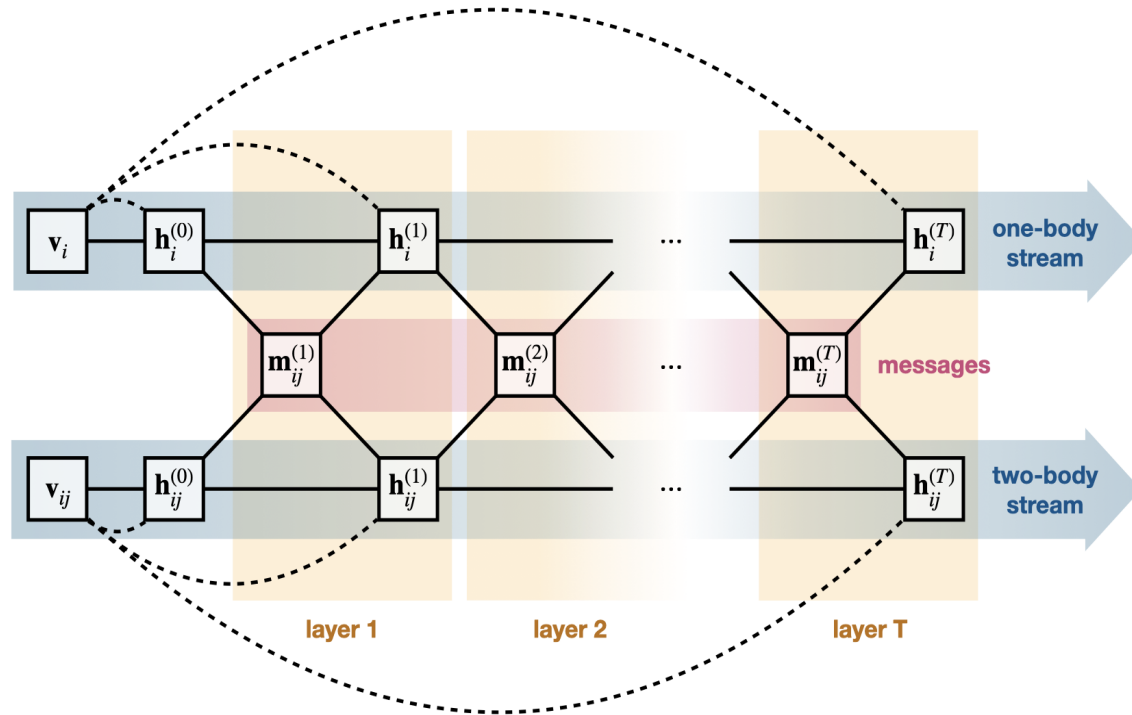
- Messages

$$\mathbf{m}_{ij}^{(t)} = \mathbf{M}_t(\mathbf{h}_i^{(t-1)}, \mathbf{h}_j^{(t-1)}, \mathbf{h}_{ij}^{(t-1)})$$

- Iteration:

$$\mathbf{h}_i^{(t)} = [\mathbf{v}_i, \mathbf{F}_t(\mathbf{h}_i^{(t-1)}, \mathbf{m}_i^{(t)})],$$

$$\mathbf{h}_{ij}^{(t)} = [\mathbf{v}_{ij}, \mathbf{G}_t(\mathbf{h}_{ij}^{(t-1)}, \mathbf{m}_{ij}^{(t)})].$$



COLD FERMION GASES

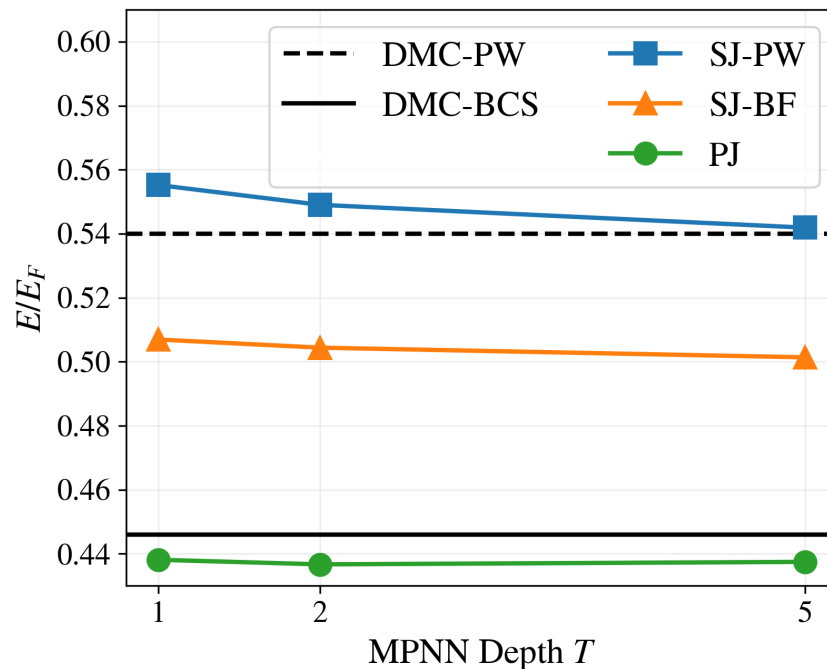
We benchmark the performances of the neural-network quantum states with DMC calculations

- Slater - Jastrow

$$e^{J(X)} \times \begin{bmatrix} \phi_1(\mathbf{x}_1) & \phi_1(\mathbf{x}_2) & \cdots & \phi_1(\mathbf{x}_N) \\ \phi_2(\mathbf{x}_1) & \phi_2(\mathbf{x}_2) & \cdots & \phi_2(\mathbf{x}_N) \\ \vdots & \vdots & \ddots & \vdots \\ \phi_N(\mathbf{x}_1) & \phi_N(\mathbf{x}_2) & \cdots & \phi_N(\mathbf{x}_N) \end{bmatrix}$$

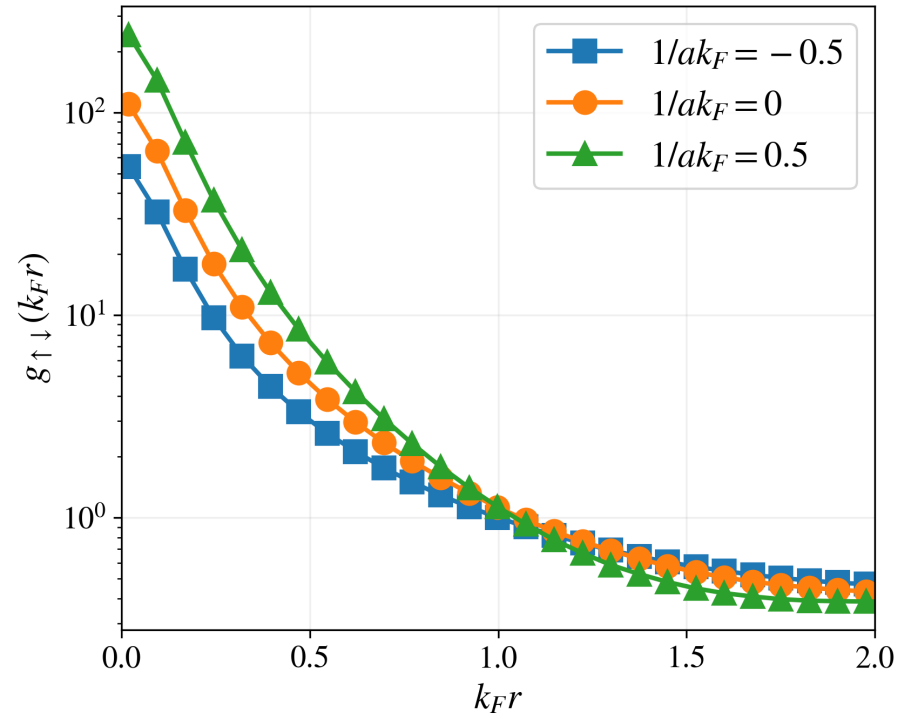
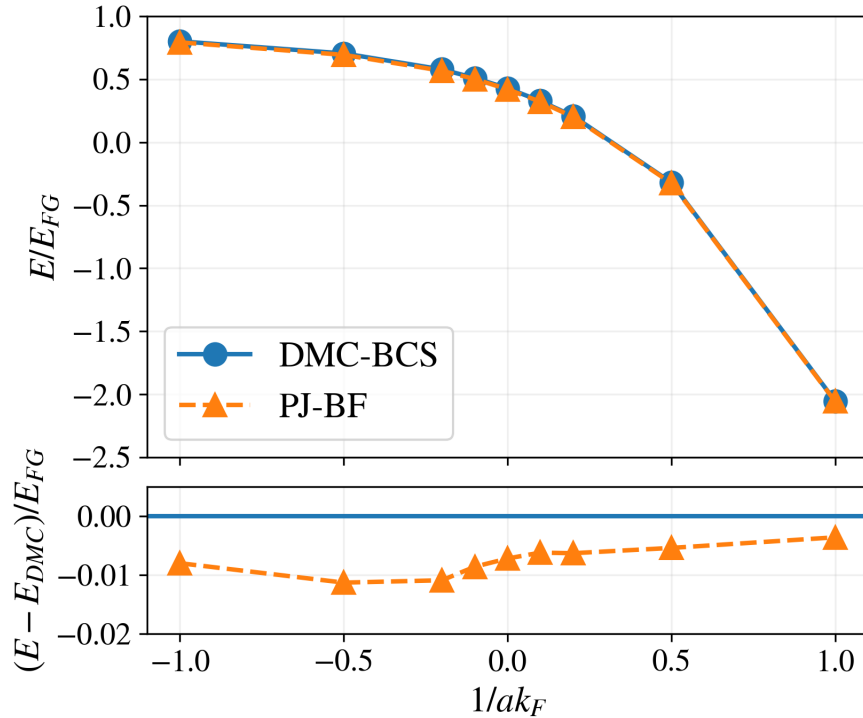
- Pfaffian - Jastrow

$$e^{J(X)} \times \text{pf} \begin{bmatrix} 0 & \phi(\mathbf{x}_1, \mathbf{x}_2) & \cdots & \phi(\mathbf{x}_1, \mathbf{x}_N) \\ \phi(\mathbf{x}_2, \mathbf{x}_1) & 0 & \cdots & \phi(\mathbf{x}_2, \mathbf{x}_N) \\ \vdots & \vdots & \ddots & \vdots \\ \phi(\mathbf{x}_N, \mathbf{x}_1) & \phi(\mathbf{x}_N, \mathbf{x}_2) & \cdots & 0 \end{bmatrix}$$



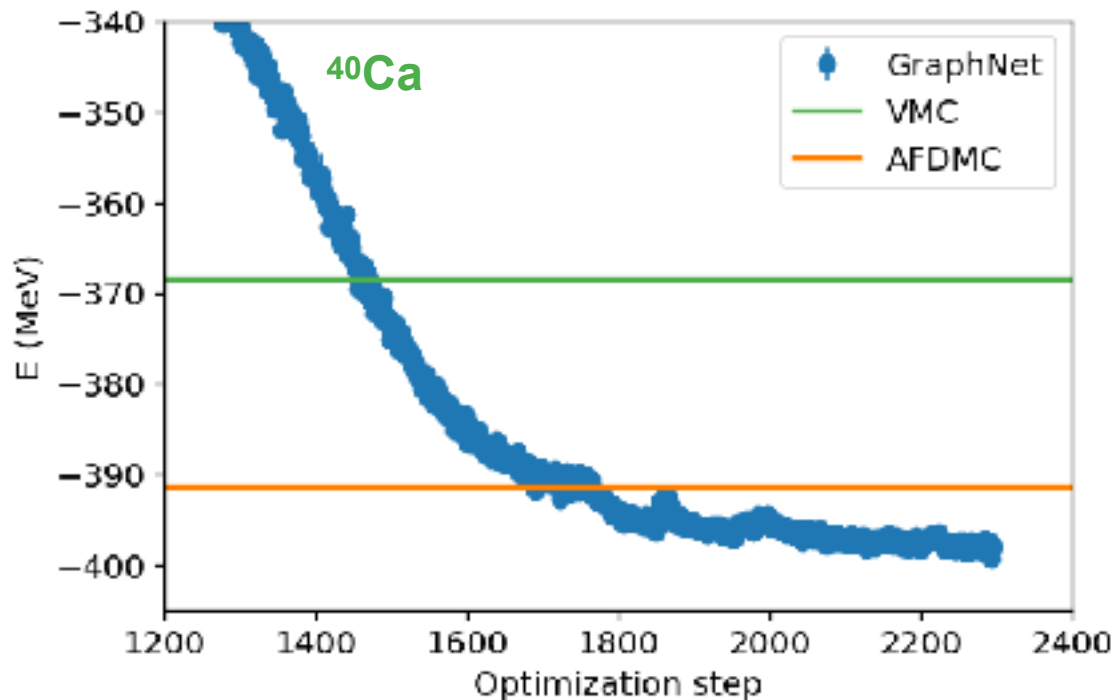
COLD FERMI GASES

We proved that neural-network quantum state can model the BCS - BEC crossover better than DMC



BACK TO NUCLEI, WITH MPNN

Even with just one hidden-nucleon we do better than AFDMC for medium-mass nuclei



CONCLUSIONS

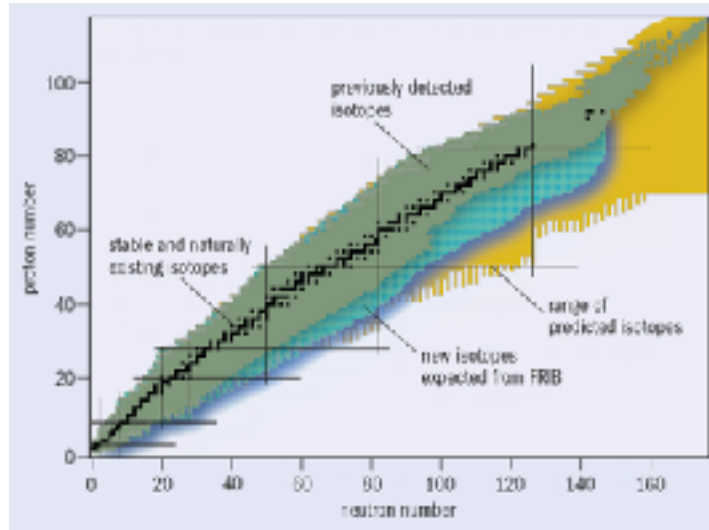
Neural network quantum states are extending the reach of conventional QMC methods

- Favorable scaling with the number of fermions;
- Universal and accurate approximations for fermion wave functions;
- Suitable for confined and periodic systems;
- Scalable to leadership-class hybrid CPU/GPU computers



PERSPECTIVES

- NQS calculations of medium-mass stable and exotic nuclei relevant to FRIB and ATLAS experiments;



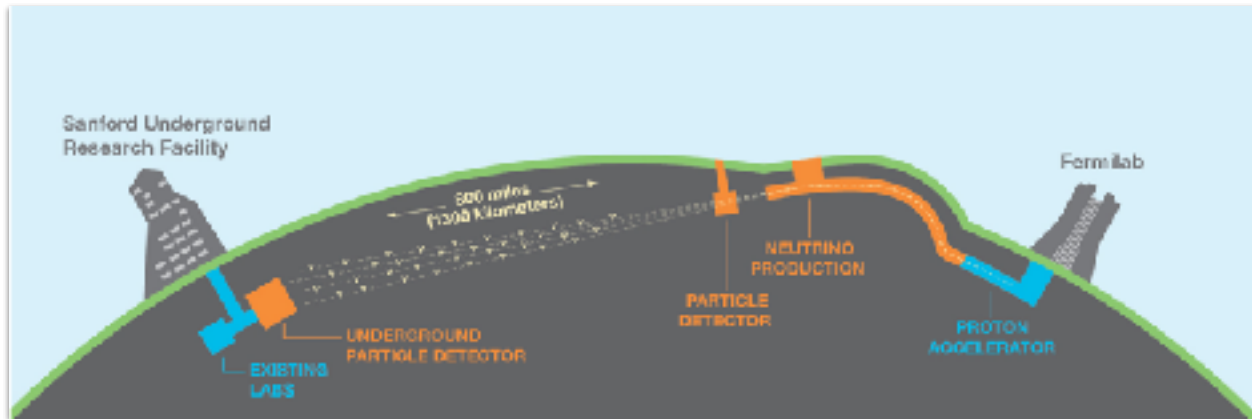
- High-precision electroweak transitions, including magnetic moments and beta-decay rates;
- Compute low-density isospin-asymmetric nucleonic matter: the flexibility of NQS will allow us to see self-emerging clustering in the low-density region;

PERSPECTIVES

- Access “real-time” dynamics: the prototypical exponentially-hard problem in many-body theory

$$\mathcal{D} (|\Psi(\mathbf{p}_{t+\delta t})\rangle, e^{-iHt}|\Psi(\mathbf{p}_t)\rangle)^2 = \arccos \left(\sqrt{\frac{\langle \Psi(\mathbf{p}_{t+\delta t}) | e^{-iHt} | \Psi(\mathbf{p}_t) \rangle \langle \Psi(\mathbf{p}_t) | e^{iHt} | \Psi(\mathbf{p}_{t+\delta t}) \rangle}{\langle \Psi(\mathbf{p}_{t+\delta t}) | \Psi(\mathbf{p}_{t+\delta t}) \rangle \langle \Psi(\mathbf{p}_t) | \Psi(\mathbf{p}_t) \rangle}} \right)^2$$

- Relevant for: fusion, lepton-nucleus scattering, and collective neutrino oscillation;



A solid green vertical bar is located on the left side of the slide, extending from the top to the bottom.

THANK YOU